POLITECNICO DI TORINO
Repository ISTITUZIONALE

Modelling non-linear interference in non-periodic and disaggregated optical network segments

(Article begins on next page)

18 October 2022

Modelling non-linear interference in non-periodic and disaggregated optical network segments

ELLIOT LONDON,[1,*] **ANDREA D'AMICO,**[1] **EMANUELE VIRGILLITO,**[1] **ANTONIO NAPOLI,**[2] **AND VITTORIO CURRI**[1]

[1]*Department of Electronics and Telecommunications, Politecnico di Torino, Corso Duca degli Abruzzi 24, 10129 Torino, Italy*
[2]*Infinera Ltd, London, UK*
*elliot.london@polito.it

Abstract: We investigate the generation of nonlinear interference (NLI) within two disaggregated transmission scenarios, each considering a chain of three distinct optical line systems that contain fibers with different dispersion values, with 400G-ZR+ 64 GBd transmission simulated using the split-step Fourier method. Firstly, by separating the NLI into its main constituents: the self- and cross-phase modulations, we investigate the impact of accumulated dispersion upon NLI generation and compensate for the coherent accumulation of the former to produce a model that is fully spectrally and spatially separable, including for alien wavelengths. Considering ideal and optimized in-line amplification, we calculate the amplified spontaneous emission noise and combine this value with the recovered NLI to obtain the generalized signal-to-noise ratio. We show that this disaggregated model provides accurate and conservative results for both transmission scenarios, showing that abstracting these signals with a Gaussian noise approximation always results in a conservative prediction, even for non-uniform fiber dispersion scenarios.

1. Introduction

The maximization of optical network capacity continues to be an important goal for network operators due to fast-growing internet traffic demands [1]. For many networks, fiber installation has represented a significant capital expenditure (CAPEX) requirement, and as such the deployment of more fiber spans is not an appealing solution to meet these capacity requirements [2]. Consequently, strategies that are able to extract additional capacity from existing infrastructures have become appealing, as these present a cost-effective way to meet these increasing demands whilst minimizing CAPEX. From a top-level and management perspective, networks have begun to move towards open and disaggregated architectures, where independent lightpaths (LPs) are transmitted across optical line systems (OLSs) that terminate in open and disaggregated reconfigurable add-drop multiplexers (ROADM)s [3,4]. This disaggregated optical network framework affords a greater degree of flexibility when compared to current aggregated networks, enabling a multi-vendor environment. In this regime, similarly open and disaggregated transmission protocols are utilized, which in turn enables the OLSs that compose the network to also be disaggregated, and their quality of transmission (QoT) estimated independently from one another. Consequently, a fully disaggregated approach that stretches from the network control plane down to the physical layer is permitted, as long as the impairments generated at the physical layer are able to be abstracted in an equally disaggregated fashion. These impairments may be separated into their linear and nonlinear contributions: the amplified spontaneous emission (ASE) noise that arises from the in-line amplifiers (ILAs), and the nonlinear interference (NLI), respectively. Concerning the former quantity, it is possible to estimate this through characterization of the ILAs, or through machine learning methods [5–7].

Accurate quantification of the NLI requires further scrutiny in a disaggregated environment, primarily due to a dependence upon the history of the LP under test. The two main contributors to the NLI are the cross-phase modulation (XPM) and self-phase modulation (SPM), which are the NLI noises generated by interfering channels and the channel under test (CUT), respectively. The SPM produces a coherent contribution to the NLI, initially preventing a spatially disaggregated approach, however the upper bound of this effect may be quantified by considering its asymptotic accumulation [8]. Using this coherency correction, the SPM may be combined with the XPM, permitting a superposition to be realized, which in turn permits all NLI contributors to be accurately computed in a spectrally and spatially separated manner [9], as required by channels with unknown parameters and history. The recovery of the total NLI in this way has been shown to be valid for periodic links, but in a realistic disaggregated optical network scenario one may expect variations in physical layer parameters between different network sections due to the aforementioned multi-vendor approach. In addition to the SPM coherency contribution, the NLI depends upon the previously accumulated dispersion, which in turn depends upon the LP history. When the LP history is partially or fully unknown, a corresponding lack of knowledge occurs concerning the NLI generation through the LP. This introduces an uncertainty which must be overcome to provide an accurate QoT estimation, which is essential for LP feasibility evaluation.

When approaching NLI modelling from an aggregated perspective, such as with implementations of the enhanced Gaussian noise model (EGN) [10], it is possible to derive fast and highly accurate closed-form approximations in point-to-point transmission configurations, given that a high level of knowledge about the system configuration is known [11,12]. In a disaggregated optical network framework a high level of knowledge about certain system parameters is not guaranteed, as vendors may be unwilling to share essential spectral or device information due to privacy reasons [13]. Additionally, a shared network infrastructure allows alien wavelengths to be present, which are channels operated by a third-party vendor that may have unknown source and/or destination nodes within the network [14]; an example network structure with already-deployed wavelengths with different transmission standards and alien wavelengths is shown in Fig. 1. As the NLI depends upon the LP history, the presence of alien wavelengths therefore presents a fundamental problem for NLI estimation. Consequently, modelling of a disaggregated optical network therefore requires the use of an equally disaggregated approach to NLI generation that is able to account for missing system information.
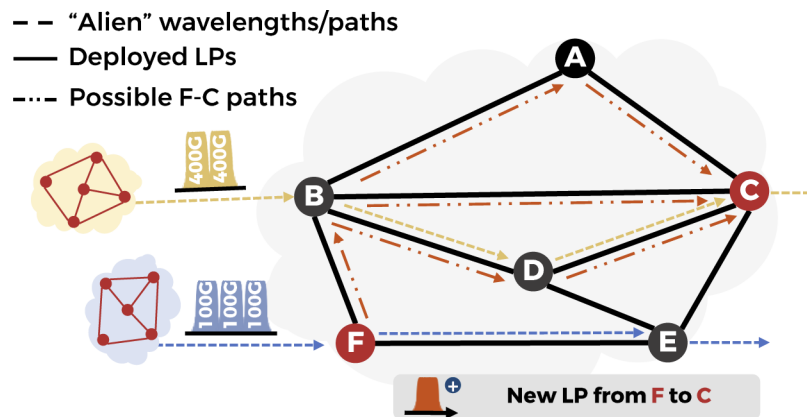
Fig. 1. New LP assignment in an example disaggregated network architecture from a network control perspective. Each labelled node represents the start/termination of an independent OLS, with alien wavelengths that exhibit different transmission parameters and originating from different, unknown sources pass through the network via different routes.

Within this work we extend the investigation performed in [15], clarifying the dependence of the NLI upon the previously accumulated dispersion over a given LP within a disaggregated network scenario. We then investigate the generation of NLI within two disaggregated optical network segments, with the OLSs within them having fiber spans with distinct dispersion values, representing a mixed fiber deployment scenario. Following this, we extend the analysis performed in [9] to this framework, investigating NLI generation in various spectral load scenarios using an internal simulation framework that solves the dual polarization Manakov equation [16], implementing a NLI model that is fully spectrally and spatially separated.

The remainder of this work is divided as follows: in Sec. 2. we outline the disaggregated network framework and describe the network abstraction under consideration. In Sec. 3. we outline the common features of the simulation framework used to investigate disaggregated NLI generation. In Sec 4. we discuss the impact of accumulated dispersion upon NLI generation, presenting the results of a simulation campaign where dispersion is progressively introduced to a single-span, pump-and-probe transmission scenario and compared to periodic transmission. In Sec. 5. we simulate transmission through two distinct network segments in terms of both NLI and GSNR, and discuss the implications from a network management perspective. This work is then concluded in Sec. 6.

2. Disaggregated optical networks

The level of disaggregation of an optical network depends upon the openness and characteristics of the low-level components and top-level management. Throughout this study we consider a framework where open re-configurable optical add-drop multiplexers (ROADM)s are used to route wavelength division multiplexed (WDM) signals through independent optical line systems (OLS)s [17,18]. Introducing these ROADMs at the ingress/egress of all OLSs permits a fully disaggregated approach; upgrades to a closed network may be progressively introduced to first progress towards a partially disaggregated architecture [19]. In a fully disaggregated scenario, a decentralized approach to network planning and management is enabled through software-defined networking (SDN) implementations: this allows LPs to be assigned dynamically and enables a higher degree of network automation [20,21]. In this framework, deployment, management and coordination of LPs is handled by optical network controllers (ONCs), who receive QoT estimations from optical line controllers (OLCs) that are correspondingly responsible for managing the physical layer and setting the working points of the ILAs.

The QoT is commonly estimated using the generalized signal-to-noise ratio (GSNR) on an LP-by-LP basis [22,23]. The GSNR has two contributors: the optical signal-to-noise ratio (OSNR), which includes all linear impairments, primarily the ASE noise generated by the amplifiers, and the nonlinear signal-to-noise ratio, (SNR_{NL}), which includes all nonlinear contributions, most prominently the NLI that is generated during fiber propagation. When modelling each LP as an additive and white Gaussian noise (AWGN) channel, the GSNRs (and corresponding OSNRs and SNR_{NL}s) of each wavelength, λ are expressed as [24]:

$$GSNR_{\lambda} = \left(OSNR_{\lambda}^{-1} + SNR_{NL;\lambda}^{-1} \right)^{-1} . \tag{1}$$

Operating within the disaggregated network paradigm, the total GSNR of a LP may be calculated as the sum of all GSNRs of each wavelength, for a LP passing through an OLS composed of N_s fiber spans of span index n:

$$GSNR = \left(\sum_{n=1}^{N_s} GSNR_{\lambda,n}^{-1} \right)^{-1} . \tag{2}$$

An example disaggregated architecture where two independent OLSs managed by two different vendors and connected to the SDN controller through separate application programming interfaces

(APIs) is shown in Fig. 2. Firstly, tackling the OSNR contribution, we assume that the ILAs are fully idealized erbium-doped fiber amplifiers (EDFAs) operating solely within the C-band, with their working points set to their optimal values by the OLC, and as such the ASE noise is the only contributor to the OSNR. In general, this is not the case, as the EDFAs have frequency dependent noise figures and gain profiles, with the latter often experiencing fluctuations [25,26], along with contributions due to other linear impairments such as filtering impairments. These effects may be included and compensated for in more in-depth amplification modelling processes [7,27,28]; in this work we focus primarily upon NLI generation, and as such these procedures lie outside of our scope. Consequently, as the ASE noise is fully linear, the OSNR may be written in terms of the power of a given CUT, P_{CUT}, and the power of the ASE noise, P_{ASE}:

$$\text{OSNR}_{\lambda,n} = \left(\sum_{n=1}^{N_s} \frac{P_{\text{ASE};\lambda}}{P_\lambda} \right)^{-1}. \tag{3}$$

Considering next the SNR_{NL} contribution, the SPM and XPM contributors to the NLI have been shown to be independent and separable for all realistic use cases [10,29,30]. Concerning disaggregation, the total NLI may be considered as fully spectrally (per-channel) separable for a wide range of use cases [9], but spatial (per-span) separability requires consideration of the coherent accumulation of the SPM. This can be achieved by calculating the asymptotic level of the coherency and subsequently using a coefficient, C_∞, to quantify the maximum amount of SPM that may be generated in a single span, for a given system configuration [8]. Including this correction, a conservative upper bound for the SNR_{NL} can be expressed as:

$$\text{SNR}_{\text{NL};\lambda,n} \leq \left(\sum_{s=1}^{N_s} \frac{\left[(1 + C_\infty) P_{\text{SPM},\lambda} + P_{\text{XPM},\lambda} \right]}{P_\lambda} \right)^{-1}, \tag{4}$$

where $P_{\text{SPM},\lambda}$ and $P_{\text{SPM},\lambda}$ are the SPM and XPM powers for a given λ, respectively. Accurately quantifying the SNR_{NL} is a problem when the LP history is unknown, which corresponds to λ having an unknown origin. Within the following sections we detail simulation campaigns that has been performed in order to investigate the impact upon SNR_{NL} in this scenario.
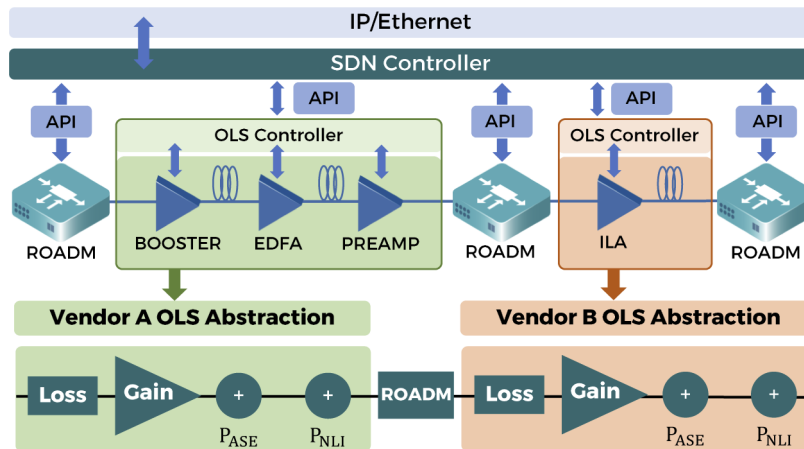
Fig. 2. Visualization of the AWGN abstraction used to model distinct, multi-vendor OLSs within a partially disaggregated optical network framework. Separately managed OLSs are connected via open and disaggregated ROADMs and connected to a decentralized SDN controller with distinct APIs.

3.   Simulation framework

For all simulations within this work we use an internal simulation framework developed in MATLAB that solves the dual polarization Manakov equation (based on [16]) for a variety of transmission and line configurations. Within this section will we outline the simulation engine workflow and features and that are common for all scenarios, with the configurations associated with specific investigations explained in following sections.

Starting on the transceiver (TRX) side, a digital signal processing (DSP)-based TRX is used to generate a dense WDM comb, with each polarization component generated using an independent pseudo-random binary sequence (PRBS) using a 15th degree polynomial. Before transmission, each channel within the WDM comb is up-sampled and shaped using a raised-cosine filter, with roll-off values for all channels set to 0.15. We consider 15 coherent channels within a 75 GHz WDM grid, with the CUT serving as the central channel, located at 193.9 THz, with 7 pumps densely packed on either side. We refer to this configuration as a reference spectral comb, as specific configurations, such as pump-and-probe simulations, are described when performed in further sections. Throughout this work we transmit signals with symbol rates of 64 Gbaud, with modulation formats and channel input powers depending upon the scenario under investigation and detailed within the two following sections.

At the receiver side, we employ a DSP-based library with multiple stages. Firstly, to isolate the CUT, the signal is passed through a re-sampling filter to isolate only the frequencies within the considered bandwidth. We then apply an ideal, noiseless analog-to-digital converter (ADC), converting the four polarization states of the signal into a digital representation. The signal is then passed to an adaptive equalizer stage which utilizes a least mean squares (LMS) algorithm with 42 taps and an adaptation coefficient, μ, of 1×10^{-4}. A large number of equalizer taps is used in order to unsure that the back-to-back (B2B) performance is high with respect to the transmitted signal, and to ensure that the NLI is recovered accurately. Next, dispersion compensation is performed, with an ideal dispersion compensation module fully recovering the dispersion that is accumulated during propagation, for all fiber spans within the line. Following this, a blind phase search carrier phase estimation (CPE) stage based upon the Viterbi algorithm [31], is performed, with the optimal memory found on a per-span basis. Subsequently, the SNR_{NL} is extracted by taking the error vector magnitude (EVM) upon the received constellation at 1 sample per symbol, at each span termination. For all line configurations these simulations are performed with ideal, transparent amplifiers, meaning that the measured SNR_{NL} directly corresponds to the GSNR. This approach is clarified when the GSNR is evaluated during Sec. 5. For all investigations within this work we present our results in terms of SNR_{NL} and ΔSNR_{NL}, which is the amount of NLI accumulated per span before CPE, and the gradient of the former value, respectively.

4.   Effect of accumulated dispersion upon disaggregated NLI generation

For our first simulation campaign we wish to investigate the impact of accumulated dispersion upon the NLI generation, in order to handle interfering channels which have an unknown or uncertain history. We perform this by comparing the results of two distinct propagation scenarios. Firstly, we have considered an OLS composed of 40 identical fiber spans with dispersion values of 16 ps / (nm·km), each followed by an ideal EDFA operating in transparency, fully recovering the fiber loss induced during propagation. Secondly, we have considered a single fiber span followed by an ideal transparent EDFA, performing signal propagation through this configuration 40 separate times, each with a different amount of predistortion applied to the pump. We start without any predistortion applied, representing a LP that originates from the TRX preceding the first fiber span. Next we transmit a signal with predistortion equal to that of one previously crossed fiber span, iterating this amount until a value representing 40 previously crossed fiber spans is reached, giving a total of 40 separate single-span simulations.

Due to the aforementioned coherency of the SPM accumulation, evaluating the XPM generated by a single interfering channel (a pump-and-probe simulation) represents the most straightforward scenario to investigate. We consider two fiber length values (50 km and 100 km) for both transmission scenarios, with a single interfering channel located at 194.05 THz (150 GHz away from the CUT). The power of the CUT (the probe) is set to $P_{CUT} = -20$ dBm in order to avoid the generation of SPM effects and isolate only the XPM contribution. The power of the interfering channel (the pump) is set to $P_{ch} = 6$ dBm, ensuring that a high level of NLI is generated, and that transmission lies deep within the nonlinear regime. The CUT has been transmitted as a polarization-multiplexed (PM)- quadrature phase shift keying (QPSK) modulated signal, whereas the pump has been launched with dual polarization (DP)-QPSK and DP-16-quadrature amplitude modulation (QAM) modulation formats. Additionally, for the single span scenario we have considered transmission of a pump with a Gaussian modulation format. These configurations were chosen to highlight the dependence of modulation format upon dispersion accumulation; we keep the CUT as DP-QPSK as this setting provided the highest level of accuracy within our simulation framework, and we observed that changing the probe modulation format had a negligible impact upon the NLI generation.

The results of this simulation campaign are presented in Fig. 3(a) and 3(b), for the DP-QPSK and DP-16-QAM modulated pump scenarios, respectively. In addition to these simulations, we have included the amount of SNR_{NL} generated in a single span using an accurate and disaggregation-enabled implementation of the Gaussian noise (GN) model [32] within the open-source GNPy library [33,34]. Firstly, it is observable that ΔSNR_{NL} is a span length dependent quantity, with a different, constant level being attained for the two different fiber lengths, for both modulation format scenarios. This difference can be primarily explained due to the differences between the effective lengths of the two fibers. As the fiber length increases, the constant level lowers and tends towards that of the Gaussian modulated pump, but never exceeding this value [15]. Secondly, for both modulation formats, the single span simulations tend towards an identical asymptote, which corresponds well to the level given by the Gaussian modulated pump, and does go below this value except for small numerical fluctuations. This behaviour can be explained as the amount of previously accumulated dispersion in the form of predistortion shaping the pump signal, causing its shape to progressively tend towards a that of a Gaussian. The level provided by the GN model serves as a theoretical upper bound on the amount of NLI that is able to be generated in a single span; a level which is equal for both modulation formats. We also observe that the amount of NLI generated within the first few (<5) fiber spans

(a)   (b)
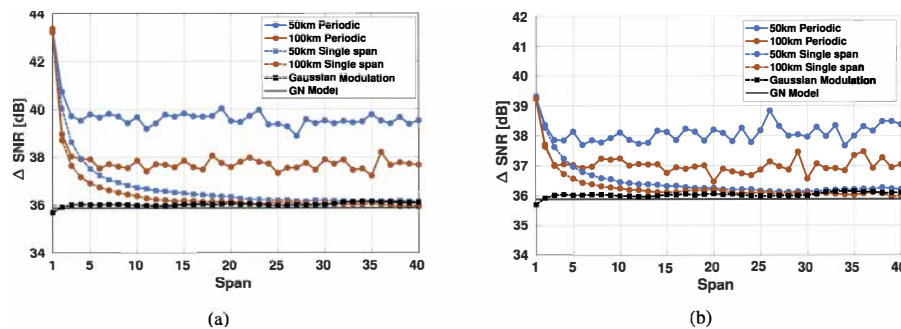
Fig. 3. The gradient of the SNR_{NL} accumulation, ΔSNR_{NL}, for a 16-QAM pump 150 GHz distant from a QPSK probe, after transparent propagation through 40 spans of SSMF fiber. The results given by the GN model, a Gaussian modulated pump, 40 periodic span propagation, and propagation through 40 single spans with varying levels of predistortion are shown.

differs between the two modulation format cases; this has been previously observed in [10,29], and may be explained by less dense constellations requiring a greater amount of predistortion to reach the worst-case Gaussian scenario. The result of this investigation is that, in the case of an unknown LP history, it is possible to place an upper bound on the amount of NLI generated in a single span by using the value provided by the GN model, or by modelling transmission of a Gaussian modulated pump.

5. Modelling disaggregated network segments

To verify the conclusion reached within the previous section we perform a second simulation campaign over two disaggregated network segments. In realistic optical network infrastructures, maintaining a constant fiber length and dispersion value for all spans within an OLS may not represent a realistic scenario, particularly in the case of a disaggregated optical network, as extensions/upgrades may not necessarily conform to existing standards. The behaviour of the NLI accumulation for network links where fiber dispersions vary significantly span-by-span has not been well explored, particularly when SPM contributions are significant and when channel histories may be unknown.

To investigate these scenarios we simulate two disaggregated network segments, each consisting of three OLSs. These OLSs each consist of 15 fibers with uniform dispersion values of 4, 8 and 16 ps / (nm·km), ordered such that the dispersion values of the fibers change every 5 spans; the ordering of these OLSs is described in Table 1. These layouts are chosen such that both a large increase and reduction in fiber dispersion from one OLS to another is experienced, from 4 to 16 ps / (nm·km for Scenario 1, and vise versa for Scenario 2). As for other fiber parameters, we maintain a constant loss coefficient of $\alpha_{dB} = 0.2$ dB/km and nonlinearity coefficient of $\gamma = 1.27$ 1/W/km for all fiber spans. For both scenarios we perform an identical simulation campaign that consists of three simulation subsets: a single-channel simulation to analyze the SPM generated upon the CUT, a full-spectrum simulation to quantify the total NLI, and a series of pump-and-probe simulations for all pumps within the full spectrum scenario, in order to individually quantify the XPM generated by each interfering channel. Following the same approach as [9], these pump-and-probe simulations may be superimposed in a disaggregated network framework, which allows a direct comparison to the NLI generated within the full-spectrum simulation.

Table 1. A summary of the two disaggregated network segments investigated within this work. Each OLS consists of 5x80 km fiber spans, each followed by a transparent amplifier.

Scenario	OLS 1	OLS 2	OLS 3
1	16 ps / (nm·km)	4 ps / (nm·km)	8 ps / (nm·km)
2	4 ps / (nm·km)	16 ps / (nm·km)	8 ps / (nm·km)

For identical reasons as the previous simulation campaign, we restrict the modulation format of the CUT to DP-QPSK and transmit all pumps with DP-16-QAM. Concerning the channel powers, for the single-channel and full-spectrum scenarios, we set all channel powers to 3 dBm. For the pump-and-probe simulations the power of the probe and pumps is scaled as follows: for the first pump, we wish to prevent crosstalk between the probe and the interfering channel, and as such use a probe power of -5.5 dBm and a pump power of 3 dBm. For the other pumps, we use a probe power of -20 dBm, and find the power of the ith pump, $P_{ch;i}$, with the following relation, in linear units:

$$P_{ch;i} = \sqrt{i \cdot P_{ch;1}} , \tag{5}$$

where $P_{ch;1}$ is 3 dBm converted into linear units. This conversion ensures that an equal amount of NLI is generated for each interfering pump, producing NLI values are significantly larger

than the simulation noise floor. All simulation results are then subsequently scaled to the local-optimization global-optimization (LOGO) power value [35], which represents the optimal system working point that is found and implemented by OLCs.

Firstly, we first present the results of Scenario 1: in Figs. 4(a), 4(b), and 4(c), we show the $\Delta \text{SNR}_{\text{NL}}$ values of the single-channel, pump-and-probe, and full-spectrum and superposition scenarios, respectively, along with the corresponding levels given by the GN model. For the single-channel results, the SPM coherency has been compensated for by calculating C_{∞} and including it within the GN model evaluation of Eq. (4). For all spans except one, this model is conservative, giving an adequately accurate prediction that increases as the number of previously crossed fiber spans grows. Moving to the pump-and-probe simulations, we present the results of 5 pumps, including the first 3 nearest to the probe. We remark that, for all interfering channels, the level provided by the GN model provides an accurate and conservative prediction, including for when fiber dispersion is changed between OLSs. Similarly, considering the full-spectrum and superposition results in Fig. 4(c), we see that the GN model remains conservative for all fiber spans, and that the superposition recovers the full spectrum well, further cementing the spatial disaggregation hypothesis. In Fig. 4(d), we show the SNR_{NL} values of the full-spectrum, superposition and GN model results, with the latter providing a consistently conservative prediction. We additionally include calculation of the OSNR, considering a that these OLSs contain amplifiers that are operating at their optimal working points; a value for all spans which is 3 dB lower than the GN model prediction. Subsequently, the GSNRs for each result are calculated using Eq. (1) – after the addition of the OSNR, the difference between the full-spectrum and
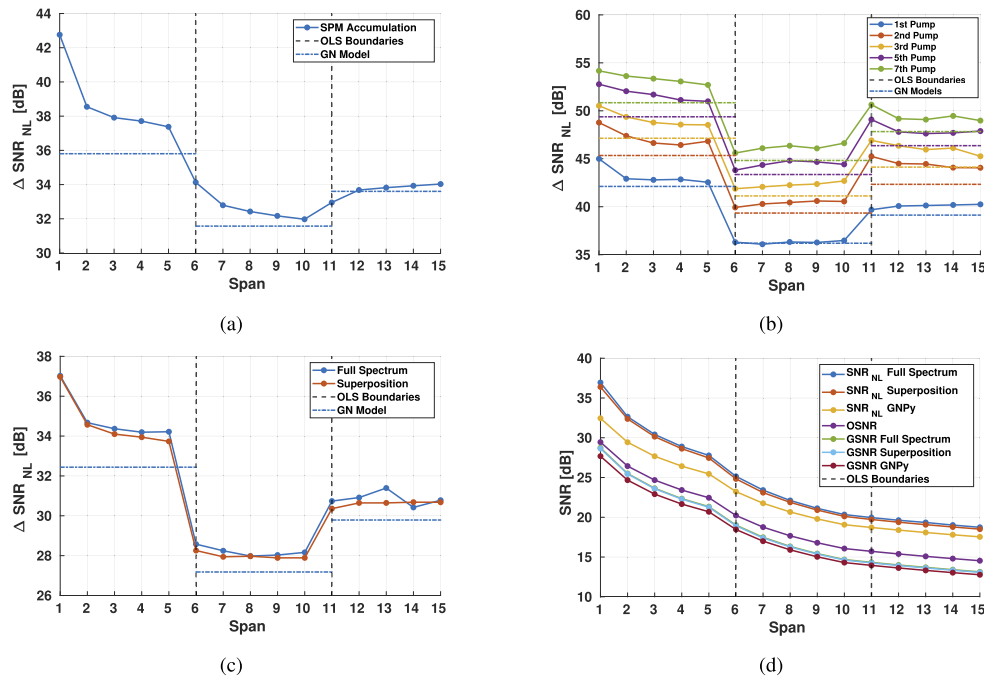
Fig. 4. The gradient of the SNR_{NL} accumulation, $\Delta \text{SNR}_{\text{NL}}$, for Scenario 1. We present: (a) a single propagating channel, (b) 5 selected pump-and-probes, (c) a full spectrum transmission scenario compared with that of a pump-and-probe superposition. In (d), the SNR_{NL} accumulation of (c) is shown, along with an OSNR calculated by considering ideal amplification, and the corresponding GSNRs for the full spectrum, superposition and GNPy simulations.

superposition is negligible, and the difference between the GN model and these results after 15 spans of propagation is approximately 0.4 dB, which represents an acceptable level of accuracy.

For completeness, we include the results of Scenario 2 in Figs. 5(a) through 5(d); identical conclusions are reached with this fiber span configuration, with a similar level of accuracy of approximately 0.6 dB between the final GSNR of the GN model and the full spectrum after 15 spans of propagation. We have observed that increasing transmission distance results in GN model predictions with a higher level of accuracy, corresponding to the signal characteristics tending towards that of a Gaussian. We remark that the accuracy of the GN model along the OLS depends primarily upon the transmission distance and the dispersion of the crossed fiber spans, with lower accuracy being found when these values are are correspondingly lower. In summary, the GN model provides an accurate and conservative upper bound upon the NLI generation for all interfering channels within the investigated scenario, with the prediction error decreasing to tolerable levels when considering the GSNR of a network segment that has been set to its optimal working point by the OLCs. Consequently, if the history of any channels within these configurations are unknown, the GN model level corresponding to the absent pump(s) could be used in place of their simulated or measured values, guaranteeing a conservative prediction, even for scenarios where the characteristics of the OLSs vary or may also be partially unknown.
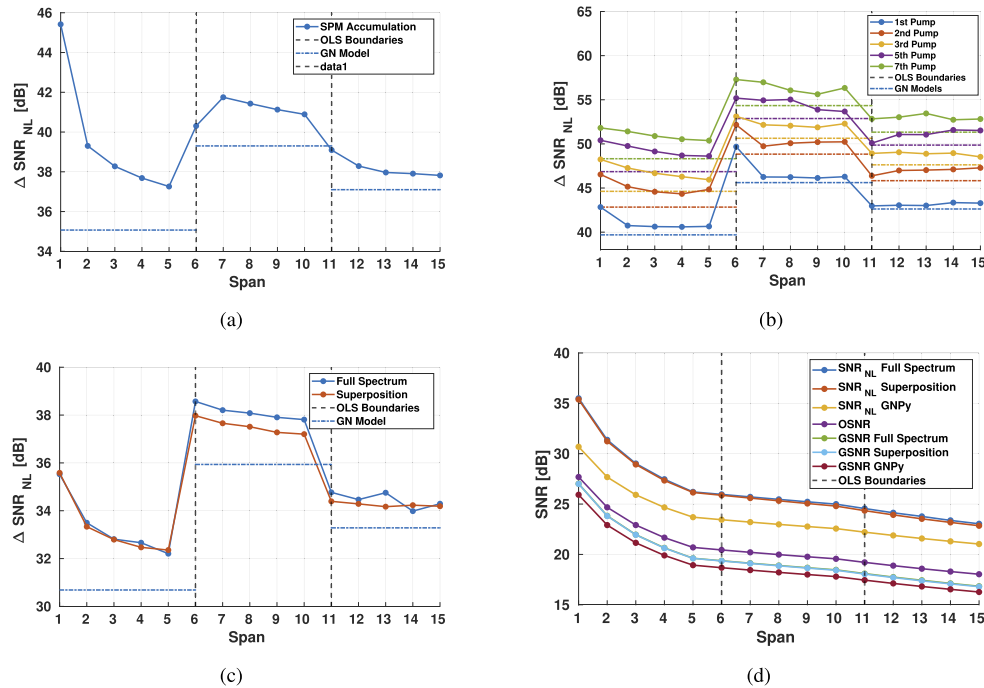
Fig. 5. The gradient of the SNR_{NL} accumulation, ΔSNR_{NL}, for Scenario 2. We present: (a) a single propagating channel, (b) 5 selected pump-and-probes, (c) a full spectrum transmission scenario compared with that of a pump-and-probe superposition. In (d), the SNR_{NL} accumulation of (c) is shown, along with an OSNR calculated by considering ideal amplification, and the corresponding GSNRs for the full spectrum, superposition and GNPy simulations.

6. Conclusion

Within this work we have evaluated NLI generation within a disaggregated network framework, presenting the results of two distinct investigations; the first concerning the effect of fiber

dispersion upon NLI generation, and the second concerning the magnitude of NLI generation within a non-uniform fiber deployment scenario. For the former, we show that the NLI of a wavelength passing through a LP with a fully unknown history corresponds well to that of a fully Gaussian pump, which is accurately approximated by the GN model. Consequently, the GN model can always be used as a conservative upper bound for interfering channels with unknown origins. Using this knowledge, we have then investigated the SPM and XPM NLI contributors within a network segment that consists of fiber spans with varying dispersion values. By accounting for the SPM coherency, we obtain accurate and conservative results for both NLI contributors, for all investigated scenarios. We then show that an accurate estimation of the NLI for a full spectrum scenario is recovered by superimposing these contributions. By considering amplifiers operating at the optimal working point, we recover GSNR values for these values and the disaggregated model, with the latter providing conservative GSNR estimations that are 0.4 and 0.6 dB lower than the corresponding simulated results, for the two disaggregated network segments under investigation. We conclude that using the GN model to estimate the maximal NLI generation for channels with unknown histories in a disaggregated network is a valid approach, additionally for OLSs containing fiber spans with variable dispersion values.

Disclosures. The authors declare no conflicts of interest.

Data Availability. Data underlying the results presented in this paper are not publicly available at this time but may be obtained from the authors upon reasonable request.

References

1. "Cisco visual networking index: Forecast and methodology," https://www.cisco.com/c/en/us/solutions/service-provider/visual-networking-index-vni/index.html (2018). [Online; accessed 11-March-2021].
2. G. Wellbrock and T. J. Xia, "How will optical transport deal with future network traffic growth?" in *2014 The European Conference on Optical Communication (ECOC)*, (IEEE, 2014), pp. 1–3.
3. K. Roberts, Q. Zhuge, I. Monga, S. Gareau, and C. Laperle, "Beyond 100 gb/s: capacity, flexibility, and network optimization," J. Opt. Commun. Netw. **9**(4), C12–C24 (2017).
4. N. Sambo, P. Castoldi, A. D'Errico, E. Riccardi, A. Pagano, M. S. Moreolo, J. M. Fabrega, D. Rafique, A. Napoli, S. Frigerio, E. H. Salas, G. Zervas, M. Nölle, J. K. Fischer, A. Lord, and J. P.-P. Gimenez, "Next generation sliceable bandwidth variable transponders," IEEE Commun. Mag. **53**(2), 163–171 (2015).
5. A. D'Amico, S. Straullu, A. Nespola, I. Khan, E. London, E. Virgillito, S. Piciaccia, A. Tanzi, G. Galimberti, and V. Curri, "Using machine learning in an open optical line system controller," J. Opt. Commun. Netw. **12**(6), C1–C11 (2020).
6. N. Sambo, Y. Pointurier, F. Cugini, L. Valcarenghi, P. Castoldi, and I. Tomkos, "Lightpath establishment assisted by offline qot estimation in transparent optical networks," J. Opt. Commun. Netw. **2**(11), 928–937 (2010).
7. A. D'Amico, S. Straullu, G. Borraccini, E. London, S. Bottacchi, S. Piciaccia, A. Tanzi, A. Nespola, G. Galimberti, S. Swail, and V. Curri, "Enhancing lightpath qot computation with machine learning in partially disaggregated optical networks," IEEE Open J. Commun. Soc. **2**, 564–574 (2021).
8. A. D'Amico, E. London, E. Virgillito, A. Napoli, and V. Curri, "Quality of transmission estimation for planning of disaggregated optical networks," in *2020 International Conference on Optical Network Design and Modeling (ONDM)*, (IEEE, 2020), pp. 1–3.
9. E. London, E. Virgillito, A. D'Amico, A. Napoli, and V. Curri, "Simulative assessment of non-linear interference generation within disaggregated optical line systems," OSA Continuum **3**(12), 3378–3389 (2020).
10. A. Carena, G. Bosco, V. Curri, Y. Jiang, P. Poggiolini, and F. Forghieri, "Egn model of non-linear fiber propagation," Opt. Express **22**(13), 16335–16362 (2014).
11. D. Semrau, E. Sillekens, P. Bayvel, and R. I. Killey, "Modeling and mitigation of fiber nonlinearity in wideband optical signal transmission," J. Opt. Commun. Netw. **12**(6), C68–C76 (2020).
12. C. Lasagni, P. Serena, and A. Bononi, "A raman-aware enhanced gn-model to estimate the modulation format dependence of the snr tilt in c+ l band," in *45th European Conference on Optical Communication (ECOC 2019)*, (IET, 2019), pp. 1–4.
13. N. Hashemi, P. Safari, B. Shariati, and J. K. Fischer, "Vertical federated learning for privacy-preserving ml model development in partially disaggregated networks," in *2021 European Conference on Optical Communication (ECOC)*, (IEEE, 2021), pp. 1–4.
14. L. Alahdab, E. Le Rouzic, C. Ware, J. Meuric, A. Triki, J.-L. Augé, and T. Marcot, "Alien wavelengths over optical transport networks," J. Opt. Commun. Netw. **10**(11), 878–888 (2018).
15. E. London, E. Virgillito, A. D'Amico, A. Napoli, and V. Curri, "Observing cross-channel NLI generation in disaggregated optical line systems," in *Asia Communications and Photonics Conference (ACP)*, (2021).

16. D. Pilori, M. Cantono, A. Carena, and V. Curri, "Ffss: The fast fiber simulator software," in *2017 19th International Conference on Transparent Optical Networks (ICTON)*, (IEEE, 2017), pp. 1–4.

17. E. Riccardi, P. Gunning, Ó. G. de Dios, M. Quagliotti, V. López, and A. Lord, "An operator view on the introduction of white boxes into optical networks," J. Lightwave Technol. **36**(15), 3062–3072 (2018).

18. J. Kundrát, O. Havliš, J. Jedlinskỳ, and J. Vojtěch, "Opening up roadms: Let us build a disaggregated open optical line system," J. Lightwave Technol. **37**(16), 4041–4051 (2019).

19. M. De Leenheer, T. Tofigh, and G. Parulkar, "Open and programmable metro networks," in *Optical Fiber Communication Conference*, (Optical Society of America, 2016), pp. Th1A–7.

20. A. de Sousa, P. Monteiro, and C. B. Lopes, "Lightpath admission control and rerouting in dynamic flex-grid optical transport networks," Networks **69**(1), 151–163 (2017).

21. D. Rafique and L. Velasco, "Machine learning for network automation: overview, architecture, and applications [invited tutorial]," J. Opt. Commun. Netw. **10**(10), D126–D143 (2018).

22. M. Filer, M. Cantono, A. Ferrari, G. Grammel, G. Galimberti, and V. Curri, "Multi-vendor experimental validation of an open source qot estimator for optical networks," J. Lightwave Technol. **36**(15), 3073–3082 (2018).

23. V. Curri, "Software-defined wdm optical transport in disaggregated open optical networks," in *2020 22nd International Conference on Transparent Optical Networks (ICTON)*, (IEEE, 2020), pp. 1–4.

24. A. Carena, G. Bosco, V. Curri, P. Poggiolini, and F. Forghieri, "Impact of the transmitted signal initial dispersion transient on the accuracy of the GN-model of non-linear propagation," in *39th European Conference and Exhibition on Optical Communication (ECOC 2013)*, (IET, 2013), pp. 1–3.

25. A. Mahajan, K. Christodoulopoulos, R. Martínez, S. Spadaro, and R. Mu noz, "Modeling edfa gain ripple and filter penalties with machine learning for accurate qot estimation," J. Lightwave Technol. **38**(9), 2616–2629 (2020).

26. A. Ferrari, G. Borraccini, and V. Curri, "Observing the generalized snr statistics induced by gain/loss uncertainties," in *45th European Conference on Optical Communication (ECOC 2019)*, (IET, 2019), pp. 1–4.

27. S. Zhu, C. Gutterman, A. D. Montiel, J. Yu, M. Ruffini, G. Zussman, and D. Kilper, "Hybrid machine learning edfa model," in *Optical Fiber Communication Conference*, (Optical Society of America, 2020), pp. T4B–4.

28. E. Seve, J. Pesic, and Y. Pointurier, "Accurate qot estimation by means of a reduction of edfa characteristics uncertainties with machine learning," in *2020 International Conference on Optical Network Design and Modeling (ONDM)*, (IEEE, 2020), pp. 1–3.

29. R. Dar, M. Feder, A. Mecozzi, and M. Shtaif, "Properties of nonlinear noise in long, dispersion-uncompensated fiber links," Opt. Express **21**(22), 25685–25699 (2013).

30. D. J. Ives, P. Bayvel, and S. J. Savory, "Adapting transmitter power and modulation format to improve optical network performance utilizing the gaussian noise model of nonlinear impairments," J. Lightwave Technol. **32**(21), 4087–4096 (2014).

31. A. Viterbi, "Nonlinear estimation of psk-modulated carrier phase with application to burst digital transmission," IEEE Trans. Inf. Theory **29**(4), 543–551 (1983).

32. P. Poggiolini, G. Bosco, A. Carena, V. Curri, Y. Jiang, and F. Forghieri, "The gn-model of fiber non-linear propagation and its applications," J. Lightwave Technol. **32**(4), 694–721 (2014).

33. "GitHub repository of GNPy," DOI: 10.5281/zenodo.3458319.

34. A. Ferrari, M. Filer, K. Balasubramanian, Y. Yin, E. Le Rouzic, J. Kundrat, G. Grammel, G. Galimberti, and V. Curri, "Gnpy: an open source application for physical layer aware open optical networks," J. Opt. Commun. Netw. **12**(6), C31–C40 (2020).

35. R. Pastorelli, S. Piciaccia, G. Galimberti, E. Self, M. Brunella, G. Calabretta, F. Forghieri, D. Siracusa, A. Zanardi, E. Salvadori, G. Bosco, A. Carena, V. Curri, and P. Poggiolini, "Optical control plane based on an analytical model of non-linear transmission effects in a self-optimized network," in *39th European Conference and Exhibition on Optical Communication (ECOC 2013)*, (IET, 2013), pp. 1–3.